Research Inventy: International Journal of Engineering And Science
Issn (e): 2278-4721, Issn (p):2319-6483, PP: 54-63
www.researchinventy.com

Optimal Design and Economic Feasibility of Grid Connected Photovoltaic Energy System using Particle Swarm Optimization

Dipak Kumar Dash[+], Pradip Kumar Sadhu*, Alok Kumar Shrivastav**
[+,*]*Department of Electrical Engineering, Indian Institute of Technology (Indian School of Mines) Dhanbad*
[**]*Department of Electrical Engineering, Techno International Batanagar*

{Corresponding author's email: [+] dipak.nitrkl@gmail.com}

Abstract- *Grid Connected Photovoltaic (GCPV) systems have gained more interest due to their modularity and environmental compatibility. This paper proposes an GCPV system to meet the demand for load on Captive's main campus. The economic and technical feasibility and system cost, safety and reliability of the proposed system are examined thoroughly. As a restricted optimisation problem the sizing of the system is implemented. The optimal quantity of proposed GCPV modules is used for Particle Swarm Optimization (PSO), with a view to extending the captive plant until 2025. Robust and reasonably accurate load forecasting models are developed and examined, including medium-term and long-term, to identify the monthly/annual load peaks from 2019 to 2025. PSO results are validated by comparison with Software like PVsyst and* PV_{GIS} *for the measurement procedure. The results showed the economic feasibility of the proposed GCPV system, and PSO's capability, given the well informed objective function, to produce better sizes than the software.*
Keywords- *Load Forecast; Grid Connected PV; Particle Swarm; PVsyst; PVGIS.*

I. Introduction

Global motives such as reducing greenhouse gases, continuous depletion of fossil fuels, and increasing prices of fossil-based power stations have led to the worldwide movement toward renewable energy sources. India is not an exception to this fact. As a result, the planned share of renewables in India is 20 % by the end of 2022 and 42 % by 2035 [1].

Among renewable sources, Photovoltaic (PV) systems have gained considerable interest in industrial, commercial, institutional, and residential applications due to their numerous advantages such as variability of size/power, long lifetime, simplicity of implementation, and high environmental compatibility. For instance, in building's-based applications, they can be installed on either facade, ground, or more commonly, on Grid Connecteds [2-10].

A successful pilot PV system installed at the Grid Connected was reported thirty years ago [11]. The work presented in [11] focused on analysing and evaluating three projects of interconnected residential applications in the United States [11]. That was a promising start, and several PV Grid Connected configurations have since been implemented [7-16].

Indian universities contribute to renewable energy sharing via Photovoltaic (PV) projects such as the 100-kW PV system at IIT Kanpur [17]. In addition, the research work in [18] has strongly recommended installing PV systems in the universities and research centres because they have suitable and available areas. Thus, Captive plant in India has decided to establish an GCPV system to reduce its load reduction and offer practical training in PV systems.

Grid Connected PV (GCPV) installations offer a number of benefits, including cost savings and investment security. This is because the price of energy generated by a GCPV system over its average lifetime can be easily calculated [5-16].

Albeit their mentioned advantages, GCPV systems have some limitations that are either site-specific or generic. The two main shortcomings are their output power quality and capital cost [5-16]. Also, the capital cost of PV systems, in general, is being reduced as their technologies and used materials become more mature [6-16]. Therefore, less impact is reported for the site-specific limitations on the development of Grid Connected PV systems [19-22].

To begin sizing the GCPV system, a large amount of data and information is required. The available area, load pattern, and climatological data are among them. The site may impose a strict constraint, such as a crowded building within the city. It is not always a constraint, as in institutions with ample space, such as universities. In either case, the load pattern will be critical for the best PV design, dictating load prediction techniques (LF).

In the short, medium and long term, LF techniques are classified according to the period considered [22-29]. A load prediction from a day to a week is identified as short-term forecasting, while from a month to an entire year is a medium-term category. If the forecasting period is about 10 to 20 years, the long-term is applied to predict the power demand [22-29]. In both long-term and medium-term LF cases, the power system's growth plan to meet the load requirements is developed. The studied system identifies not just that, but also the economic and social developments.

Different applied LF systems include statistical, mathematical, artificial and smart methods, as well as regression analysis[22-29]. Furthermore, the LF has recently made use of heuristic optimization techniques. These methods are probabilistic, which means they can correctly identify the best global solution with the fewest demands.

PSO is a meta-heuristic approach that is widely used in which the particles adapt their journey according to their experiences and experience. PSO has some merits, such as simplicity of implementation, quick convergence, and relatively low computational requirements [30-33].

Here, the core contributions of this paper are claimed as:

- Developing both medium- and long-term LF models characterized by simplicity, reliability, and robustness. Such models are an essential tool for the optimal sizing of the proposed GCPV system.
- Development of an optimal design approach of the GCPV system considering the constraints, such as available area and power flow to and from the power grid and achieving the problem objectives such as cost minimization and fulfilment of load requirements.
- Providing a systematic approach to examine the economic feasibility of the proposed GCPV system.

II. Brief Description of PSO Technique

The PSO technique is applied in two stages in the presented work: load forecasting and optimal sizing. Therefore, a brief description of the PSO technique is shown here [30-33].

- A swarm is formed as a uniform distribution.
- Every particle represents a possible solution related to the individuals' best performing and the whole group.
- The formed objective function is exploited to transfer from a place to another in the created search space.
- Several iterations are required for the particle to converge toward an optimal solution. Of course, such iterations vary from one problem to another according to the solution requirements.

The above procedure is formulated mathematically and is given here through equations from (1) to (4). After identifying the number of swarms and iterations, the particles are distributed randomly through the search space. The velocity of a particle in the swarm is expressed in (1) at the iteration number k+1 as:

$$v_i^{k+1} = \begin{Bmatrix} w_i v_i^k + c_1 rand\left(pbest_i^k - s_i^k\right) + \\ c_2 rand\left(gbest - s_i^k\right) \end{Bmatrix} \quad (1)$$

$$s_i^{k+1} = s_i^k + v_i^{k+1} \quad (2)$$

At each iteration, the value of the objective function is estimated and then compared to $pbest_i^k$. Also, $pbest_i^k$ is compared to *gbest*. This procedure is done to develop the performance of particles. If any particle attains a better position than *gbest*, then the number of such particles and their better positions are stored. Consequently, *gbest* is updated. This procedure lasts until the global best solution is obtained or the programmed extreme of iteration numbers is reached.

J_i is specified by [28] as,

$$J_i = J_{i\max} - \frac{J_{i\max} - J_{i\min}}{T_{i\max}} T_i \quad (3)$$

Where $J_{i\min}$ and $J_{i\max}$ represent the minimum and maximum weights, T_i and $T_{i\max}$ are the current and maximum iterative times, respectively. w_i is usually assigned within the range from 0.40 to 0.90 [31]. Thus, the maximum velocity of particle i, $v_{max,}$ is obtained via (4) as:

$$v_i^{k+1} = \begin{cases} v_i^{k+1} & \left|v_i^{k+1}\right| \text{p } v_{\max} \\ v_{\max} & v_i^{k+1} \geq v_{\max} \\ -v_{\max} & v_i^{k+1} \leq -v_{\max} \end{cases} \quad (4)$$

The described PSO algorithm is applied in the load predicting and sizing phases of the proposed GCPV installation. Finally, in Section III, a brief description of the load forecasting models is presented.

III. Models of Load Forecasting (LF)

It is critical to plan the power system for future load growth. In this context, reliable LF models for detecting the proposed system's maximum monthly and annual loads up to 2025 should be developed. Both medium- and long-term models are adapted in this study.

Albeit its stochastic nature, the load demand can be determined generally by (5) as:

$$W(t) = G_E(t) + H_N(t) \quad (5)$$

G_E(t) and W(t) are the estimated and actual load in a definite period, respectively. The term H_N(t) represents a noise component that signifies the deviation between the estimated and actual values.

2.1. Long-term Forecasting

In Section I, it was pointed out that various strategies are employed for load forecasting. This research applies the time series. Briefly, a time series is a string of numerical data points in chronological order. The authors of [30] present a model based on linear regression whose parameters are identified via a constrained PSO algorithm. So does the proposed work.

The predicted load $Y_E(k)$ for a definite period, k, is given by:

$$Y_E(k) = \sum_{i=1}^{4} a_i Y(k-i) \quad (6)$$

The constants a_i (i from 1 to 4) are provided in Table A1(in the appendix) during the interval from 2019 to 2025.

2.2. Suggested Objective Function for Long-Term LF

The LF parameters are obtained by solving the PSO problem. As suggested by (7) at which Least Square method is applied [15,28]:

$$f = \left\{ \begin{array}{l} \min\left(\sum_{k=1}^{N} [E(k)]^2\right) \\ \min\left(\sum_{k=1}^{N} [Y(k) - Y_E(k)]^2\right) \end{array} \right\} \quad (7)$$

The parameters described by equations (5), (6), and (7) are included in a constrained optimization problem, where their upper and lower limits are considered constraints, as in eq. (8):

$$f \text{ subject to } L_{\text{lower}} \leq a_{\text{paramters}} \leq L_{\text{upper}} \quad (8)$$

Where f is regarded as the objective function, L_{upper} and L_{lower} are the upper and the lower bounds of the parameters, respectively. In equation (8), the $a_{parameters}$ represent the optimized parameters. The Table II presents the load data of the campus.

2.3. Medium-term LF

The viability of the proposed GCPV system necessitates the monthly values of the estimated load. The work presented in [34] has developed a medium-term LF model, and this research suggests a modification to such a model.

The model presented in [34] was a bit unclear and got some bugs. Most importantly, it is limited to a particular system. Consequently, the suggested medium-term model in this research aims to remedy these imperfections. A block diagram of the proposed model is depicted in Fig. 1. First, Y_{Ei} and Y_i are estimated, and actual load values at the i^{th} time interval. Then, the proposed model is briefly described in the subsequent steps.

1. The yearly estimated $Y_{ETotali}$ real load and Y_{Totali} total load are calculated by:

$$Y_{ETotali} = \sum_{k=1}^{N} Y_{Ei}(k) \quad (9)$$

$$Y_{Totali} = \sum_{k=1}^{N} Y_i(k) \quad (10)$$

N denotes the number of years. The random component R_N is computed by (5), and its aggregate value, $R_{totali,}$ is calculated for N points, as the case with Y_{Totali}.

2. Then, the squares of load's data for a year, $Y_{Totalsi,}$ is found as:

$$Y_{Totalsi} = \sum_{k=1}^{N} Y_i^2(k) \quad (11)$$

Hence, $Y_{\text{Totalsi+1}}$ is estimated from Y_{Totalsi} using extrapolation.

3. The component $R_{\text{Ni+1}}$ of the next period is estimated by (12):

$$R_{Ni+1} = \sqrt{\frac{R_{Totalsi+1}}{R_{Totalsi}}} R_{Ni} \tag{12}$$

Where $R_{\text{Totalsi+1}}$ is calculated in terms of $Y_{\text{Totalsi+1}}$ and Signal to Distortion Ratio (SDR) as in eq. (13):

$$R_{Totalsi+1} = Y_{Totalsi+1} \times 10^{-SDR/10} \quad \text{and}$$

$$SDR = 10\log_{10}\left(\frac{Y_{\text{Totalsi}}}{R_{\text{Totali}}}\right) \tag{13}$$

4. Lastly, the predicted amount of load for the next period is obtained via eq. (14):

$$Y_{Ei+1} = \sqrt{\frac{Y_{Totali}}{Y_{ETotali}}}\left(Y_{Ei} + R_{Ni+1}\right) \tag{14}$$

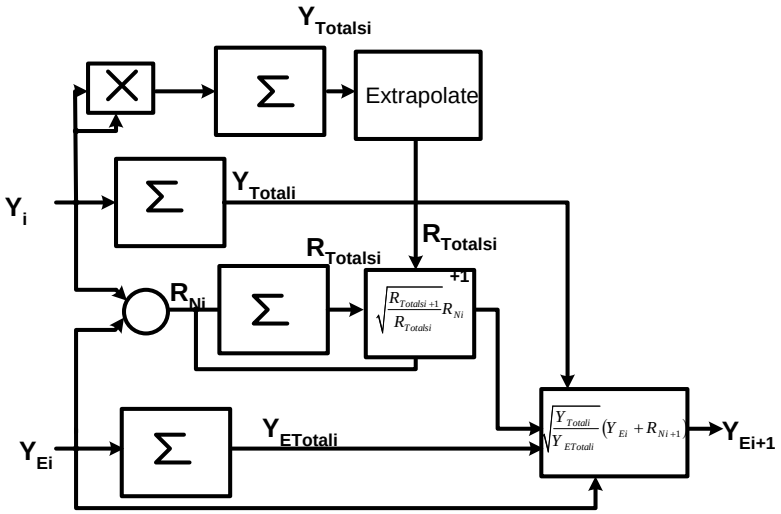

Figure 1. Logic diagram of suggested LF model.

2.4. Outcomes of LF models

Fig.2 displays the findings obtained by using the developed LF models. A substantial correlation between the informed and predicted loads is observed by comparing the data presented in Table A2 and displayed results in Fig. 2.

Hence, the proposed LF models can predict the maximum load accurately. The model's accuracy has been examined through the percentage of the absolute value of the normalized error, ε, [31] given in eq. (15):

$$\varepsilon = \frac{|Y_E - Y|}{Y} \times 100 \tag{15}$$

Due to the limited available data, calculations of the error ε were limited to a year. The results are displayed in Fig.3. The error does not exceed 9.5%, which is satisfactory for forecasting models [22-29].

IV. Structural and Technical Boundaries of the Suggested GCPV Configuration

The plan of the main campus of Captive plant is depicted in the appendix in Fig. A1. Also, the solar map of India is displayed in Fig. A2 [45], and an example of the weather forecast for India is shown in Fig. A3 [46]. The campus has approximately an area of 1.5 km^2. The curves of daily- and the monthly- load requirements are displayed in Figures 4 and 5, respectively [44.].

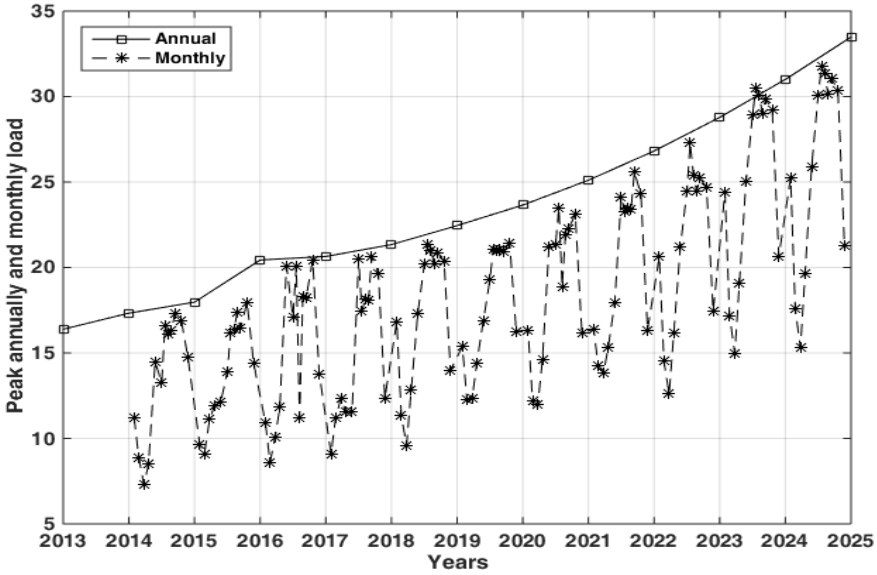

Fig. 2. Peak annual (square) and monthly (*) loads in MW.

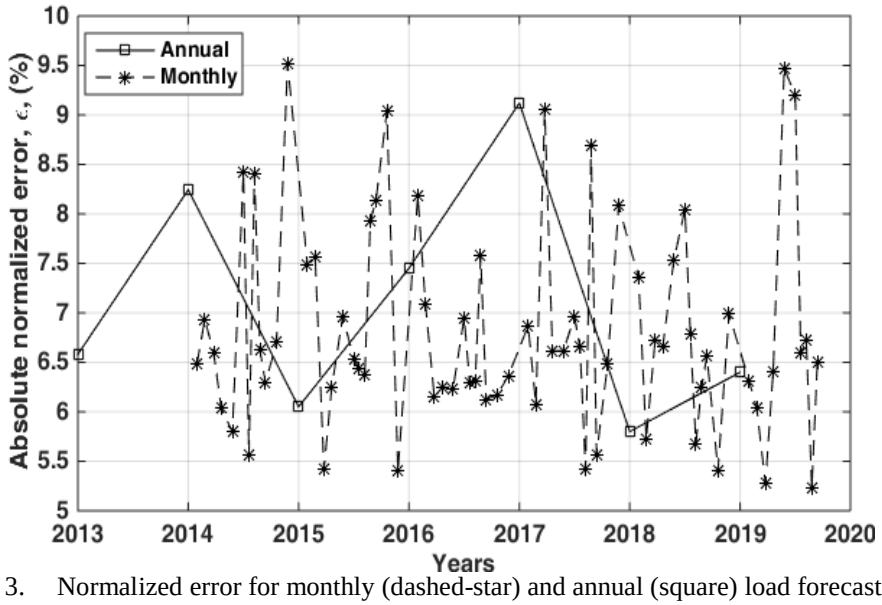

Fig. 3. Normalized error for monthly (dashed-star) and annual (square) load forecasting

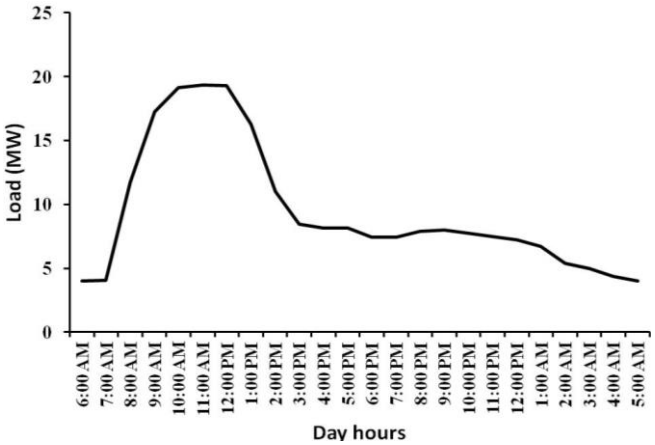

Fig. 4. Variation of daily load of Captive plant (main campus) on June 3 2018.

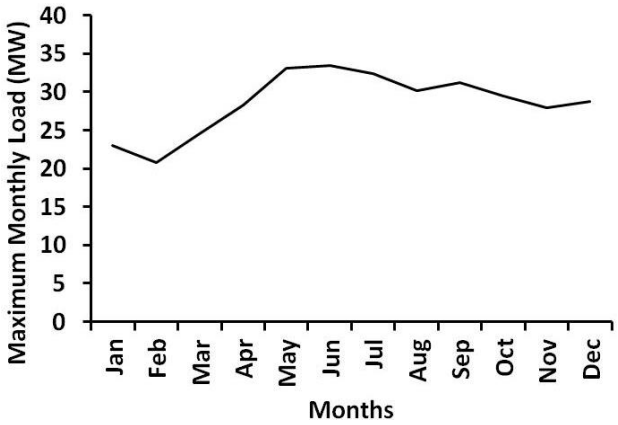

Fig.5. Peak values of the monthly load of Captive plant main campus for the year 2018.

Figures 4 and 5 reveal that the peak loads occur from 11.00 am to 2.00 pm in summer. Fig. 4 indicates that the campus's load decreases to about 25% of the peak value from 2.00 to 6.00 pm. At that time, the proposed GCPV would be operational and generating a considerable amount of power.

V. Sizing of the GCPV system

5.1 Available Areas

Here, the GCPV system's sizing is realized via the formulation of a constrained optimization problem using the PSO. The PSO algorithm outcomes are compared with the sizing procedure used using the available online Software such as PVsyst and PVGIS [31-34].

Table I. Available Areas for the RTPV

	Name	**Area available for GCPV connection, m^2**
Faculties	Engineering	14345
	Education	1200
	Arts	1931
	Science	3861
	Commerce & Lows	2500
	Agriculture	1512
	Athletic Education	3360
Supplementary buildings	University Farm	74511
	Seleman Hozien Hall	638
	Other buildings	37523
	Sum of available area	**150,000 m^2**

5.2 Objective Function for Optimal Sizing

The function f_{ob} is selected to minimize the total cost of the GCPV system whilst satisfying the load requirements fully or partially [47]:

$$f_{\mathrm{ob}} = C_{\mathrm{cap}} + C_{\mathrm{om}} + C_{\mathrm{Rp}} - C_{\mathrm{Rt}} \tag{16}$$

Where C_{cap}, C_{om}, C_{Rp} and C_{Rt} are the cost of capital, running and maintenance, and recovery. The capital cost of the GCPV installation is estimated using (17):

$$C_{\mathrm{cap}} = G_{\max} \times C_{\mathrm{PVW}} \times N_{\mathrm{PV}} \times \xi_{\mathrm{con}} + C_{\mathrm{con}} \times N_{\mathrm{con}} \times P_{\mathrm{con}} \tag{17}$$

Where: C_{PVW} and C_{con} are assigned for the prices of 1Watt peak of PVs, P_{con} is the converter power, $G_{\max}$ is the solar irradiance, and ξ_{con} is the efficiency of PVs.

The annual operation and maintenance fee is expressed in eq. (18).

$$C_{\mathrm{om}} = G_{\mathrm{PVi}} + C_{\mathrm{PVm}} \times R_{\mathrm{fPV}} + C_{\mathrm{conm}} \times R_{\mathrm{fcon}} + C_{\mathrm{coni}} \tag{18}$$

Where: C_{Pvi} is the initial cost of PV modules, C_{pvm} is the maintenance cost of PV modules, C_{coni} is the initial cost of converters, C_{conm} is the maintenance cost of a converter, R_{fpv} is the PV reduction factor, and R_{fcon} is a reduction factor of converters.

As the PV technologies are rapidly advancing, there is a continuous decline in PV components' prices. Generally, the reduction factor is calculated using eq. (19):

$$U_{\mathrm{f}} = \frac{1}{(y+1)^k} \tag{19}$$

In eq. (19), y represents the interest rate. The exponent k = 1/D where D is the time of the project. The interest rate r is specified by:

$$y = \frac{U - b}{b + 1} \tag{20}$$

In eq. (20), U represents the interest rate, and b designates the annual inflation rate.

The replacement fee, C_{Rp} is only valid if the project lifetime is longer than its components [36]. The replacement cost is calculated using (21)

$$C_{\mathrm{Rp}} = N_{\mathrm{PV}} \times C_{\mathrm{PV\text{-}Rp}} + N_{\mathrm{con}} \times C_{\mathrm{con\text{-}Rp}} \tag{21}$$

Where $C_{\mathrm{pv-Rp}}$ and $C_{\mathrm{con-Rp}}$ are the replacement fees for a PV unit and a converter, respectively.

VI. Feasibility of the GCPV structure

As stated earlier, the objectives of the optimal sizing of the GCPV system are to determine the lowest cost to fulfil the load requirement entirely (Figures 4 and 5) and confine it with the accessible areas in Table I. Nevertheless, such objectives with these limitations could be challenging to fulfil. So, two scenarios are considered for the optimization problem. Case 1 aims to have an optimal PV arrangement that confines available areas in Table I and does not wholly fulfil the full load requirements. Case 2 targets an optimal PV layout and ensures the complete contentment to the connected loads until 2025.

The GCPV system proposed is a PV type grid-connected system. Hence, the excess of generated energy will be injected into India's power grid. Conversely, the grid feeds the campus loads during low- or non-irradiance.

VII. Results and Discussions

Each scenario requires the solution of the sizing process (17). But the solution of (17) necessitates identifying the values of ξ_{con}, which widely vary according to the technology of the selected PV modules. Therefore, the research work comprised four different types of PV systems. Tables II and III show the results. Three of the adapted four types are Mono-Crystalline (MC) types, while the fourth belongs to the Poly-Crystalline (PC) type. In addition, literature such as [38-41] has reported the data of these selected modules.

7.1 optimal PV layout subjected to area limitation

The PSO algorithm in this case minimises fob function and limits it to the area accessible (Table I). The optimised design of each pv type maximises the output power of the GCPV system. [38-41]. Table II illustrates the results obtained in scenario 1.

Table II shows that the estimated power for the campus available area ranges from 22 to 28.6 MW. Moreover, the Type I module [38] achieves the minimum cost compared to the other three PV module types.

Type II module costs approximately 10.5% greater than that of Type I in the cost per 1kWp. However, the Type III module [39] offers the maximum power density (kW/m^2). As a result, it harvests 30% (approximately) higher power than the Type I PV module. Such a high-power density of Type III module may, of course, overwhelm its comparatively high cost.

Since the planned GCPV system is networked, the grid power would flow bidirectionally in accordance with the discrepancy between demand for load and possible power from the PV system. The PV and grid power amounts are depicted in Fig. 6 for a month and in Fig.7 for a whole year when using the Type III PV module.

Table II. Quantities of Inverters and PV Modules in scenario 1.

Module type	**MC-Type I [38]**	**MC –Type II [39]**	**MC –Type III [40]**	**PC-Type IV [41]**
Efficiency (%)	18.3	21.1	18.55	17.2
No. of PV Modules	77305	86845	91984	75604
No. of inverters	20	24	26	20
Max. Power (MW)	22.0	26.4	28.6	22.0
Total cost (M USD)	12.82	21.07	19.7	13.97
Cost (USD/kWp)	0.583	0.798	0.688	0.6348

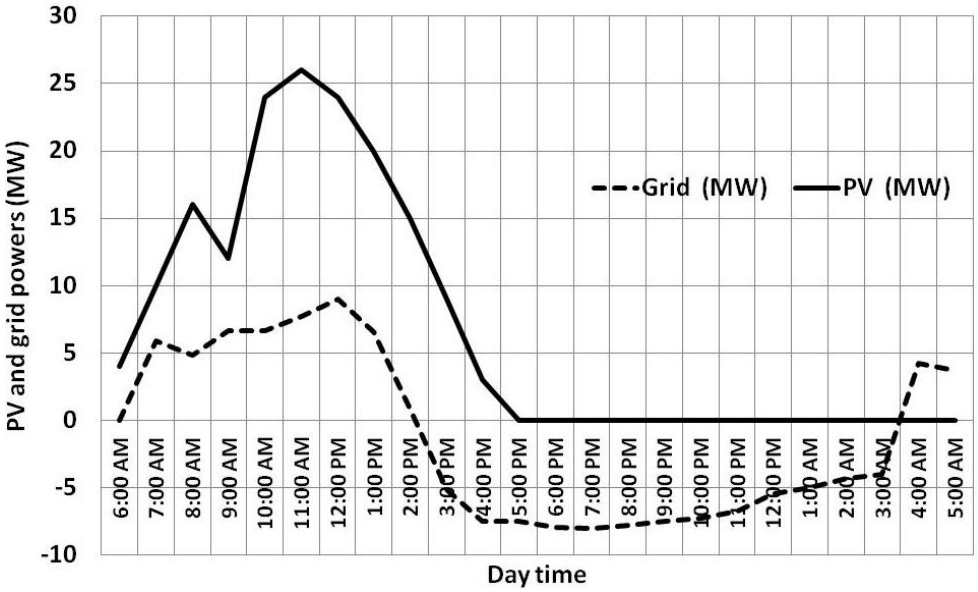

Fig. 6. Grid power (dashed) and PV power (sold) on June 3, 2021.

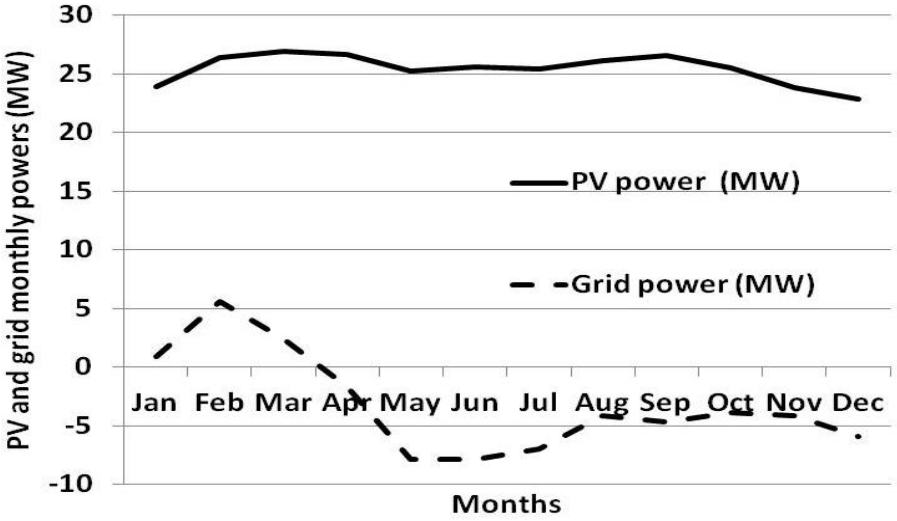

Fig.7. Grid power (dashed) and PV power (sold) for the year 2021.

It should not be overlooked that from Figures 6 and 7 solar irradiance data were obtained [40]. Fig.6 illustrates that the planned GCPV system completely satisfies the load demand from 6.00 am to 2.30 pm. The country electrical grid has to share the load with the PV system from 2.30 to 5.00 pm. Naturally, the load is only fed by the power grid at night. Fig.7 shows that the recommended GCPV system is economically possible despite limited space available, as it almost satisfies the demand for load.

VIII. Conclusions

The GCPV system was designed to meet the load demand of the Captive Plant's main campus. The sizing process, on the other hand, necessitates determining the load demand in the coming years. As a result, two load forecasting models have been developed and tested: medium-term and long-term. The procedures for load forecasting and sizing are both formulated as constrained optimization problems.The formed optimization problems were solved using the PSO algorithm. The solution to the load forecasting problem implies the estimation of load demand till the year 2025. The solution to the sizing optimization problem, on the other hand, yields the most cost-effective and power-dense PV configuration. The obtained results demonstrated the proposed GCPV's economic viability.

References

[1]. L. D. Le Nguyen et al., "Facade Integrated Photovoltaic Systems: Potential Applications for Commercial Building in Vietnam," 2019 International Conference on System Science and Engineering (ICSSE), Dong Hoi, Vietnam, 2019, pp. 219-223, DOI: 10.1109/ICSSE.2019.8823134.

[2]. D. S. Schiera, F. D. Minuto, L. Bottaccioli, R. Borchiellini and A. Lanzini, "Analysis of Grid Connected Photovoltaics Diffusion in Energy Community Buildings by a Novel GIS- and Agent-Based Modeling Co-Simulation Platform," in IEEE Access, vol. 7, pp. 93404-93432, 2019, doi: 10.1109/ACCESS.2019.2927446.

[3]. Daniele Salvatore Schiera, Luca Barbierato, Andrea Lanzini, Romano Borchiellini, Enrico Pons, Ettore Francesco Bompard, Edoardo Patti, Enrico Macii, Lorenzo Bottaccioli, "A Distributed Platform for Multi-modelling Co-simulations of Smart Building Energy Behaviour", Environment and Electrical Engineering and 2020 IEEE Industrial and Commercial Power Systems Europe (EEEIC / I&CPS Europe) 2020 IEEE International Conference on, pp. 1-6, 2020.

[4]. L. X. W. Hesselink and E. J. L. Chappin, "Adoption of energy efficient technologies by households—Barriers policies and agent-based modelling studies", Renew. Sustain. Energy Rev., vol. 99, pp. 29-41, Jan. 2019.

[5]. Y. R. Golive et al., "Analysis of Field Degradation Rates Observed in All-India Survey of Photovoltaic Module Reliability 2018," in IEEE Journal of Photovoltaics, vol. 10, no. 2, pp. 560-567, March 2020, doi: 10.1109/JPHOTOV.2019.2954777.

[6]. Yashi Singh, Bhim Singh, Sukumar Mishra, "Control of Multiple PV Integrated Parallel Inverters for Microgrid Applications", Power Instrumentation Control and Computing (PICC) 2020 International Conference on, pp. 1-6, 2020.

[7]. G. Saxena and D. L. Gidwani, "Estimation of Energy Production of Grid Connected Rooftop Solar Photovoltaic System at Nagar Nigam Kota, Rajasthan," 2018 3rd International Innovative Applications of Computational Intelligence on Power, Energy and Controls with their Impact on Humanity (CIPECH), Ghaziabad, India, 2018, pp. 45-49.

[8]. Mahmoud Dhimish, Nigel Schofield, Ayman Attya, "Insights on the Degradation and Performance of 3000 Photovoltaic Installations of Various Technologies Across the United Kingdom", Industrial Informatics IEEE Transactions on, vol. 17, no. 9, pp. 5919-5926, 2021.

[9]. A. Jasuan, Z. Nawawi and H. Samaulah, "Comparative Analysis of Applications Off-Grid PV System and On-Grid PV System for Households in Indonesia," 2018 International Conference on Electrical Engineering and Computer Science (ICECOS), Pangkal Pinang, 2018, pp. 253-258.

[10]. B. Tangwiwat and K. Audomvongseree, "Benefit and Cost Analysis of the Installation of Rooftop Solar PV with Battery System," 2018 15th International Conference on Electrical Engineering/Electronics, Computer, Telecommunications and Information Technology (ECTI-CON), Chiang Rai, Thailand, 2018, pp. 505-508.

[11]. R. Torquato, D. Salles, C. Oriente Pereira, P. C. M. Meira, and W. Freitas, "A Comprehensive Assessment of PV Hosting Capacity on Low-Voltage Distribution Systems," in IEEE Transactions on Power Delivery, Vol. 33, no. 2, pp. 1002-1012, April 2018.

[12]. S. Chattopadhyay et al., "Correlating infra-red thermography with electrical degradation of PV Modules inspected in All-India Survey of Photovoltaic Module Reliability 2016", IEEE J. Photovolt., vol. 8, no. 6, pp. 1800-1808, Nov. 2018.

[13]. N. M. kumar, M. S. P. Subathra and J. E. Moses, "Small Scale Rooftop Solar PV Systems for Rural Electrification in India," 2018 4th International Conference on Electrical Energy Systems (ICEES), Chennai, 2018, pp. 611-615.

[14]. A. Argüello, J. D. Lara, J. D. Rojas and G. Valverde, "Impact of Grid Connected PV Integration in Distribution Systems Considering Socioeconomic Factors," in IEEE Systems Journal, vol. 12, no. 4, pp. 3531-3542, Dec. 2018, doi: 10.1109/JSYST.2017.2739022.

[15]. Nand K. Singh, M.Z.C. Wanik, Abdullah A. Jabbar, Antonio Sanfilippo, "Enhancing PV hosting Capacity of a Qatar Remote Farm Network using Inverters Ability to Regulate Reactive Power-a Case Study", Innovative Smart Grid Technologies Europe (ISGT-Europe) 2019 IEEE PES, pp. 1-5, 2019.

[16]. C. P. Mediwaththe and L. Blackhall, "Network-Aware Demand-Side Management Framework With A Community Energy Storage System Considering Voltage Constraints," in IEEE Transactions on Power Systems, vol. 36, no. 2, pp. 1229-1238, March 2021, doi: 10.1109/TPWRS.2020.3015218.

[17]. S. Sewchurran, I. E. Davidson and O. Ojo, "Drivers, barriers and a method for evaluating the feasibility of residential rooftop solar PV in Durban (Part 1)," 2017 IEEE PES Power Africa, Accra, 2017, pp. 208-213, 2017.

[18]. L. Callegaro, G. Konstantinou, C. A. Rojas, N. F. Avila and J. E. Fletcher, "Testing Evidence and Analysis of Rooftop PV Inverters Response to Grid Disturbances," in IEEE Journal of Photovoltaics, vol. 10, no. 6, pp. 1882-1891, Nov. 2020, doi: 10.1109/JPHOTOV.2020.3014873.

[19]. L. Jinlian, Z. Yufen and L. Jiaxuan, "Long and medium term power load forecasting based on a combination model of GMDH, PSO and LSSVM," 2017 29th Chinese Control And Decision Conference (CCDC), Chongqing, 2017, pp. 964-969.

[20]. Kioni Ndirangu, Leonardo Callegaro, John E. Fletcher, Georgios Konstantinou, "Development of an Aggregation Tool for PV Inverter Response to Frequency Disturbances across a Distribution Feeder", Industrial Electronics Society (IECON) 2020 The 46th Annual Conference of the IEEE, pp. 4037-4042, 2020.

[21]. J. Haoran, C. Xinru, L. Yang, F. Xiaofeng, L. Shixiang and L. Guoying, "Research on Medium and Long Term Power Load Forecasting Considering Intelligent Power Utilization," 2018 China International Conference on Electricity Distribution (CICED), Tianjin, 2018, pp. 2938-2942.

[22]. X. Wenbo, S. Jia, X. Weidong, Y. Dawei, L. Zheng and Z. Jin, "The model combination method of power system load forecasting based on freshness availability index," 2017 2nd International Conference on Power and Renewable Energy (ICPRE), Chengdu, 2017, pp. 585-588.

[23]. Y. Song et al., "Medium and long term load forecasting considering the uncertainty of distributed installed capacity of photovoltaic generation," 2018 13th IEEE Conference on Industrial Electronics and Applications (ICIEA), Wuhan, 2018, pp. 1691-1696.

[24]. G. Dudek and P. Pelka, "Medium-term electric energy demand forecasting using Nadaraya-Watson estimator," 2017 18th International Scientific Conference on Electric Power Engineering (EPE), Kouty nad Desnou, 2017, pp. 1-6.

[25]. E. İlseven and M. Göl, "Medium-term electricity demand forecasting based on MARS," 2017 IEEE PES Innovative Smart Grid Technologies Conference Europe (ISGT-Europe), Torino, 2017, pp. 1-6.

[26]. L. Jinlian, Z. Yufen and L. Jiaxuan, "Long and medium term power load forecasting based on a combination model of GMDH, PSO and LSSVM," 2017 29th Chinese Control And Decision Conference (CCDC), Chongqing, 2017, pp. 964-969.

[27]. A. A. A. Hafez and M. K. Elsherbiny, "Particle swarm optimization for long-term Demand Forecasting," 2016 Eighteenth International Middle East Power Systems Conference (MEPCON), Cairo, 2016, pp. 179-183.

[28]. G. Ren, S. Wen, Z. Yan, R. Hu, Z. Zeng and Y. Cao, "Power load forecasting based on support vector machine and particle swarm optimization," 2016 12th World Congress on Intelligent Control and Automation (WCICA), Guilin, 2016, pp. 2003-2008.

[29]. G. Ji, S. Li, Z. Shi, X. Zhang and W. Zhao, "Regional Power Load Forecasting Based on PSOSVM," 2018 IEEE 4th Information Technology and Mechatronics Engineering Conference (ITOEC), Chongqing, China, 2018, pp. 1685-1688.

[30]. N. Abu-Shikhah1, F. Elkarmi1 and O. M. Aloquili" Medium-Term Electric Load Forecasting Using Multivariable Linear and Non-Linear Regression" Journal of Smart Grid and Renewable Energy, Vol. 2, pp. 126-135, 2011.
[31]. G. H. Yordanov, "Relative efficiency revealed: Equations for k1–k6of the PVGIS model," 2014 IEEE 40th Photovoltaic Specialist Conference (PVSC), Denver, CO, 2014, pp. 1393-1398.
[32]. M. L. Markovic and R. M. Ciric, "Efficiency analysis of grid-connected photovoltaic power plants," in CSEE Journal of Power and Energy Systems, Vol. 3, no. 3, pp. 269-277, Sept. 2017.
[33]. H. Hamouche and M. M. Shabat, "Sizing of a Photovoltaic LED Street Lighting System with PVsyst Software," 2019 IEEE 7th Palestinian International Conference on Electrical and Computer Engineering (PICECE), Gaza, Palestine, 2019, pp. 1-5
[34]. H. M. de Oliveira and E. de Aguiar Sodré, "Study of a grid-tied photovoltaic system in Caruaru using PVsyst and Skelion," 2018 Simposio Brasileiro de Sistemas Eletricos (SBSE), Niteroi, 2018, pp.1-6.
[35]. Yasser F. Nassar, Mohammad J. Abdunnabi, Mohamed N. Sbeta, Ahmad A. Hafez, Khaled A. Amer, Abdulaziz Y. Ahmed, Basim Belgasim, 2021. Dynamic analysis and sizing optimization of a pumped hydroelectric storage-integrated hybrid PV/Wind system: A case study, Energy Conversion and Management 229. https://doi.org/10.1016/j.enconman.2020.113744.

Appendixes

TABLE A1. Parameters of Load Forecasting Models from 2019 to 2025

Years	**2019**	**2020**	**2021**	**2022**	**2023**	**2025**
a_1	0.7378	0.45982	0.7075	0.9639	0.6806	0.8400
a_2	0.3200	0.4508	0.4533	0.8838	0.3470	0.8514
a_3	0.4685	0.1240	0.4109	0.2617	0.3199	0.4198
a_4	0.6580	0.650	0.5087	0.4450	0.5800	0.4573

Table A2. Maximum load (MW) for THE MAIN Campus of Captive plant

Year / Month	2014	2015	2016	2017	2018
Janaury	8.90	9.10	8.60	11.21	11.32
Febraury	7.30	11.10	10.10	12.40	9.60
March	8.50	11.90	11.85	11.55	12.82
April	14.47	12.13	20.10	11.50	17.30
May	13.30	13.90	17.08	20.50	20.18
June	16.60	17.37	**20.08**	17.42	**21.33**
July	16.10	16.13	11.238	18.18	21.02
August	16.30	16.35	18.27	18.08	20.13
September	**17.47**	16.44	18.23	**20.65**	20.86
October	16.89	**17.97**	21.65	19.66	20.37
November	14.32	14.42	13.78	12.36	13.99
December	11.25	9.650	10.92	9.10	16.83